Fig. 8

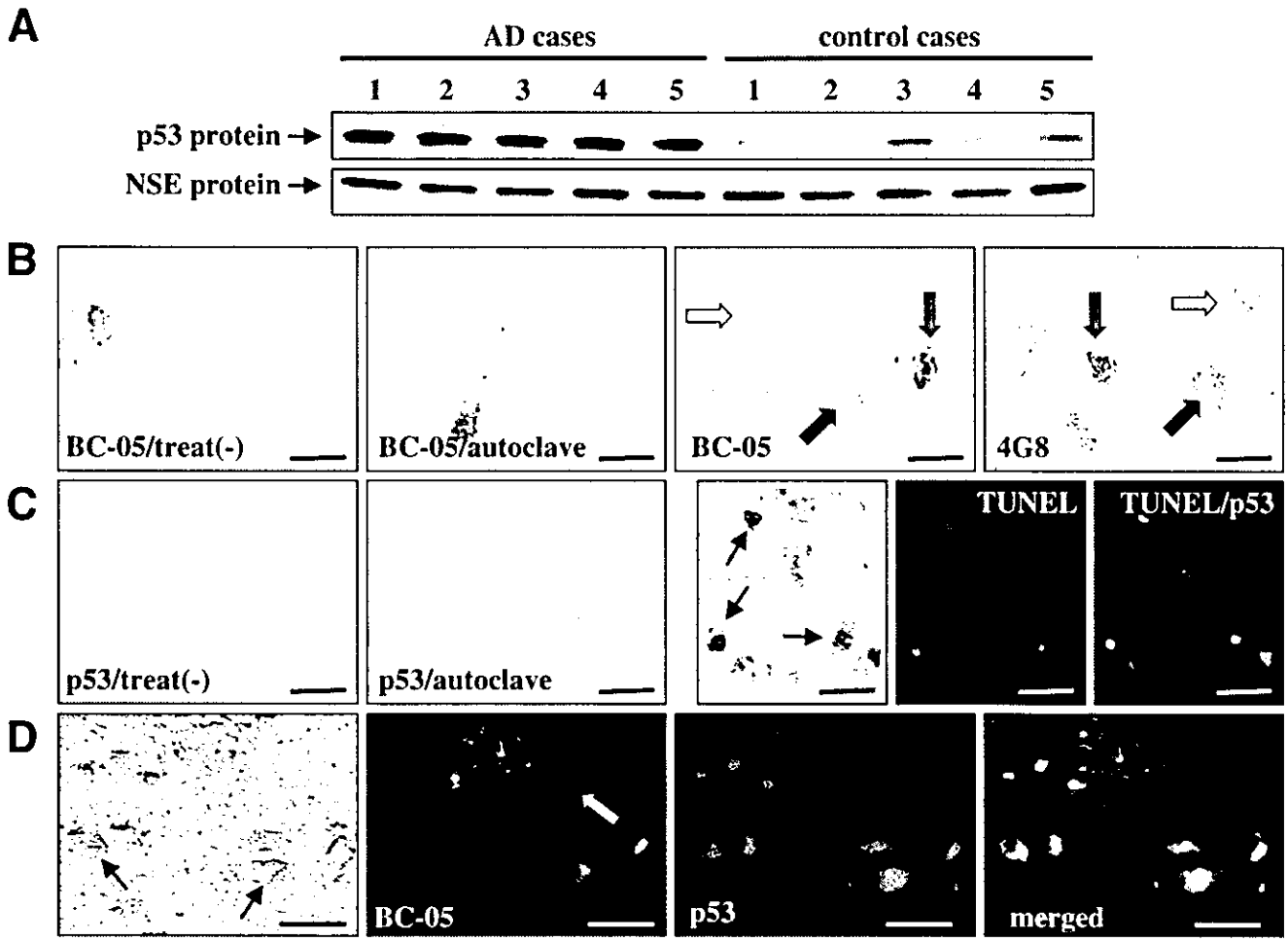

Figure 8. Immunoblotting analysis, immunocytochemical staining, and double immunostaining of AD brain tissue (temporal cortices). ***A***) P53 and NSE in the frontal cortices of 5 AD and 5 normal cases. The immunoblotting images of p53 and NSE are from the same gel. ***B***) BC-05 staining without or with autoclaving and higher magnification of BC-05 or 4G8 staining. Red arrows indicate markedly immunopositive neurons that appear to be degenerating; blue arrows indicate cytosolic granular immunopositive neurons, and white arrows indicate immunonegative neurons that look healthy. Scale bars, 20 (***right two panels***) and 50 μm (***left two panels***). ***C***) P53 staining (FL393) without or with autoclaving, and double immunostaining of p53 and TUNEL staining. Overlapping of TUNEL (green) and p53 (red) shows yellow. Scale bars, 20 (***right three panels***) and 50 μm (***left two panels***). ***D***) Overlapping of p53 (FL393, red) and Aβ42 immunoreactivity (BC-05, green) in some cells in AD brain. Black arrows indicate neurons positive for both antibodies, and white arrows indicate extracellular Aβ42 deposition that is negative for p53. Scale bars, 20 μm.

Amino-truncated amyloid β-peptide (Aβ5-40/42) produced from caspase-cleaved amyloid precursor protein is deposited in Alzheimer's disease brain

KAZUYA TAKEDA,*,† WATARU ARAKI,†,[1] HARUHIKO AKIYAMA,‡ AND TAKESHI TABIRA*,[1]

*Department of Vascular Dementia Research, National Institute for Longevity Sciences, NCGG, Obu, Japan; †Department of Demyelinating Disease and Aging, National Institute of Neuroscience, NCNP, Kodaira, Japan; and ‡Tokyo Institute of Psychiatry, Tokyo, Japan

To read the full text of this article, go to http://www.fasebj.org/cgi/doi/10.1096/fj.03-1070fje; doi: 10.1096/fj.03-1070fje

SPECIFIC AIMS

Caspase activation and apoptosis are implicated in neuronal death in Alzheimer's disease (AD). We analyzed the effects of the caspase-mediated cleavage of amyloid precursor protein (APP) on amyloid β-peptide (Aβ) production with special consideration of the generation of amino-terminally truncated Aβ.

PRINCIPAL FINDINGS

1. Evidence for altered Aβ generation from cells expressing caspase-cleaved form of APP

APP is cleaved by caspases in its cytoplasmic domain, subsequently generating APP lacking C-terminal 31 amino acids (APPΔC). Human neuroblastoma SH-SY5Y cells stably transfected with wild-type APP or APPΔC were established and designated SH-APP and SH-APPΔC cells, respectively. We selected two pairs of SH-APP and SH-APPΔC cells expressing similar APP levels (designated SH-APP-1, -2, and SH-APPΔC-1, -2 cells). SH-APP-2 and SH-APPΔC-2 expressed ~ twice as much APP as did SH-APP-1 and SH-APPΔC-1. Two types of sandwich ELISA were used to measure Aβ in conditioned media from these cells. BNT77-based ELISA detected N-terminal-intact and truncated Aβ (Aβ40total and Aβ42total), but not Aβ17-40 (p3 fragment); BAN50-based ELISA detected only N-terminal-intact Aβ (mainly Aβ1-40 and Aβ1-42). BNT77-based ELISA showed that SH-APP and SH-APPΔC cells secreted comparable levels of Aβ40total and Aβ42total. BAN50-based ELISA revealed that the amounts of Aβ1-40 and Aβ1-42 in SH-APPΔC cells were decreased to ~30% of those found in SH-APP cells. These data suggest that N-terminally truncated Aβ is increased relative to total Aβ in SH-APPΔC cells.

We next analyzed C-terminal fragments (CTF) of APP by immunoprecipitation Western blot with 4G8 antibody. Two CTF bands (~10 kDa α-CTF and ~12 kDa β-CTF) and a faint band (β′-CTF, ~11 kDa) were detected in cell lysates of SH-APP. Similarly, two bands (~6 kDa α-CTFΔC and ~8 kDa β-CTFΔC) and a faint band (β′-CTFΔC, ~7 kDa) were observed in SH-APPΔC cell samples. The relative level of β′-CTFΔC was increased in SH-APPΔC cells. Steady-state levels of β-CTFΔC and α-CTFΔC in SH-APPΔC cells were lower than those of β-CTF and α-CTF in SH-APP cells.

We compared the generation of secreted APP (sAPP) in SH-APP and SH-APPΔC cells. Immunoprecipitation Western blot showed that levels of total sAPP and sAPP-α (sAPP derived from α-secretase cleavage) were ~4-fold higher in SH-APPΔC cells, compared with SH-APP cells.

2. Increased production of amino-truncated Aβ from caspase-cleaved APP

We then analyzed altered Aβ secretion in SH-APPΔC cells using immunoprecipitation Western blot. BAN50 antibody immunoprecipitated Aβ1-40 and Aβ1-42 (band 1, comigrating with synthetic Aβ1-40/42). These immunoreactivities were decreased in media from SH-APPΔC cells, compared with SH-APP cell media. N-terminal-intact Aβ (Aβ1-40 and Aβ1-42) and the smaller fragment (band 3, most likely Aβ11-40 and Aβ11-42) were detected in media from SH-APP cells by BNT77 immunoprecipitation. In contrast, the intensities of bands 1 and 3 were reduced, and the intensity of band 2 was increased in SH-APPΔC media (**Fig. 1A**). We did not observe any band comigrating with Aβ17-40 (p3 fragment) in the BNT77 immunoprecipitates.

To identify secreted Aβ species, BNT77 immunoprecipitates were analyzed using a matrix-assisted laser desorption/ionization time-of-flight mass spectrometer (MALDI-TOF-MS). Two major peaks of Aβ1-40 and Aβ11-40 were detected in conditioned media from

[1] Correspondence: E-mail: araki@ncnp.go.jp; tabira@nils.go.jp

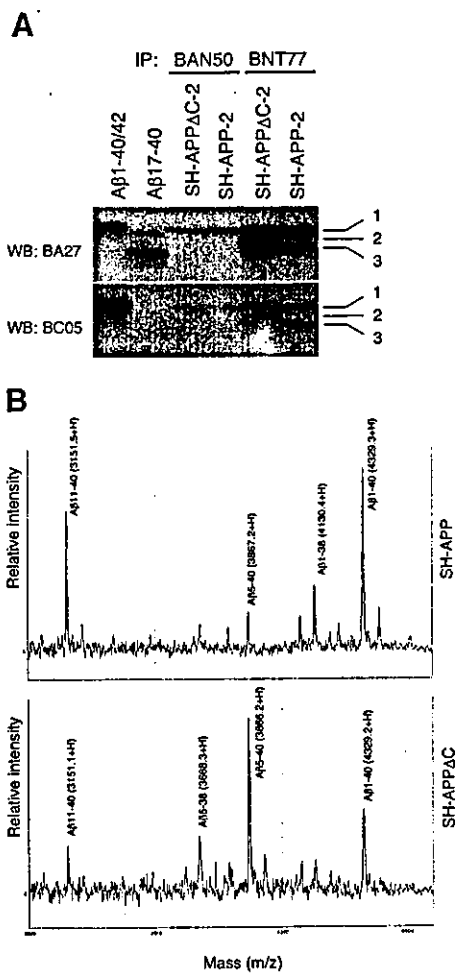

Figure 1. Immunoprecipitation Western blot and mass spectrometric analyses of secreted Aβ. *A)* Secreted Aβ peptides were immunoprecipitated with BAN50 or BNT77 antibodies and subjected to Tris-Tricine SDS-PAGE and Western blot analyses with BA27 or BC05. Synthetic Aβ1-40/42 and Aβ17-40 were simultaneously electrophoresed as markers. In BNT77 immunoprecipitates, 3 bands were detected. Band 1 corresponded to N-terminally intact Aβ1-40/42 and band 3 possibly represented Aβ11-40/42. Bands 1 and 3 were the major Aβ species in SH-APP cells. Conversely, in SH-APPΔC cells, the intensity of band 2 was markedly increased whereas that of bands 1 and 3 was reduced. In BAN50 immunoprecipitates, only band 1 was detected. *B)* Secreted Aβ was immunoprecipitated with BNT77 from conditioned media of SH-APP or SH-APPΔC cells and analyzed by MALDI-TOF-MS. Peaks were identified according to observed molecular and theoretical masses of Aβ and its variants. Aβ1-40, Aβ11-40, and some C-terminally truncated Aβ forms such as Aβ1-38 were identified in the sample from SH-APP (upper). Peak intensities of Aβ1-40 and Aβ11-40 were reduced whereas that of Aβ5-40 was markedly increased in the SH-APPΔC sample (lower). Aβ5–38 was also seen in this sample.

SH-APP cells. In contrast, the relative peak intensity of Aβ5-40 was markedly increased, whereas peak intensities of Aβ1-40 and Aβ11-40 were decreased in SH-APPΔC media (Fig. 1*B*). These data show that N-terminally truncated Aβ (starting at Arg5) is markedly increased in media from SH-APPΔC cells. Aβ11-40/42 appears to be generated through processing of APP by BACE1 and γ-secretase, as BACE1 alternatively cleaves between Tyr10-Glu11 in the Aβ sequence. Increased levels of Aβ5-40 and decreased levels of Aβ1-40 and Aβ11-40 were observed in media from HEK293 cells transiently transfected with APPΔC, compared with those transfected with APP.

We further analyzed the levels and species of intracellular Aβ in SH-APP and SH-APPΔC cells by sensitive Western blot. Aβ1-40 and Aβ1-42 levels were comparable between samples from SH-APP and SH-APPΔC cells. The intracellular Aβ1-42/Aβ1-40 ratio was ~0.4 in both cell lines. These results suggest that the generation of intracellular Aβ is unaffected by the C-terminal truncation of APP.

3. Aβ5-40/42 generation involves altered β cleavage of APP

To determine the processing mechanism by which Aβ5-40/42 is generated from APPΔC, we treated SH-APPΔC and SH-APP cells with a specific inhibitor of BACE, OM99-2. Secreted Aβ was analyzed by immunoprecipitation Western blot and mass spectrometry. In OM99-2-treated SH-APPΔC cells, Aβ1-40 secretion was significantly decreased, but the Aβ5-40 level was not altered compared with that in untreated cells. SH-APP cells treated with the inhibitor secreted significantly reduced Aβ1-40 and increased Aβ5-40 levels. These data suggest that cleavage between Phe4 and Arg5 is not mediated by BACE1. BACE1 inhibition promotes the secretion of Aβ5-40. To establish whether α-secretase-like proteases are responsible for Aβ5-40/42 generation, we incubated SH-APPΔC cells with a TACE (tumor necrosis factor-α converting enzyme) inhibitor, TAPI-1, which inhibits α-secretase. Incubation with 20 μM TAPI-1 resulted in increased Aβ1-40 and decreased Aβ5-40 secretion, suggesting that α-secretase-like proteases are involved in Aβ5-40/42 production.

4. Immunohistochemical analysis of Aβ5-40/42 in AD brain

To determine whether Aβ5-40/42 is present in human brain tissues, we generated a specific antibody to the N-terminal end region of this Aβ species (designated the Aβ5 antibody). In Western blot analyses, the Aβ5 antibody reacted with Aβ5-40, but not with Aβ1-40, whereas the BAN50 antibody recognized only Aβ1-40. The Aβ5 antibody immunostained vessels in the AD brain, indicating the deposition of Aβ5-40/42, particularly in vascular lesions with amyloid angiopathy. In nearby sections, another Aβ antibody (6E10) labeled more vessels than did the Aβ5 antibody. Amyloid angiopathy in the smaller sized vessels tended to be negative or weakly positive for Aβ5. In addition, Aβ5 antibody stained numerous neurofibrillary tangles (NFT), suggesting that Aβ5-40/42 may be deposited in the NFT. Although a small number of senile plaques were positive for Aβ5 in some cases, the staining was not as consistent as that of vessels and NFT.

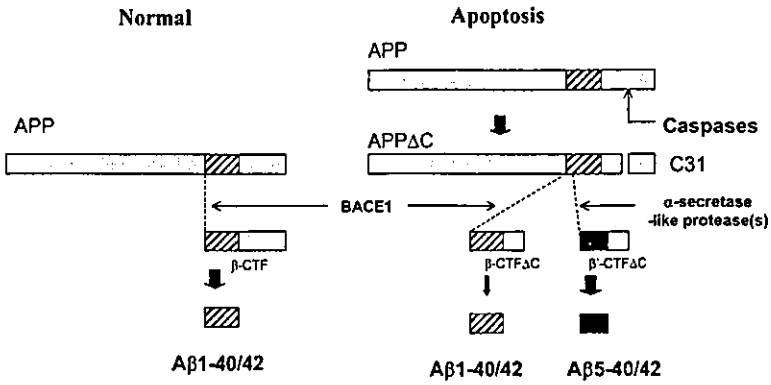

Figure 2. The possible mechanism of the generation of Aβ5-40/42. During apoptosis, APP is cleaved by caspases to form APPΔC and a C-terminal fragment consisting of 31 amino acids (C31). APPΔC is preferentially processed between Phe4 and Arg5 to generate β'-CTFΔC possibly through alternative processing by α-secretase-like protease(s). Subsequent γ-secretase cleavage results in the formation of Aβ5-40/42.

5. Cleavage at the Aβ5 site occurs when wild-type APP-expressing cells undergo apoptosis

Finally, we investigated whether APP processing to generate Aβ5-40/42 occurs during apoptosis of wild-type APP-expressing cells. SH-APP cells were exposed to MG132 or MG132 plus staurosporine. Western blots using an AB5942 antibody specific for the caspase-generated neo epitope of APP reveal that exposure to these agents leads to caspase-mediated cleavage at the cytoplasmic region of APP. We examined CTF production from caspase-processed APP by immunoprecipitation Western blot analysis with 4G8 and AB5942 antibodies. Cells treated with MG132 plus staurosporine contained significant amounts of β-CTFΔC, β'-CTFΔC, and α-CTFΔC, consistent with data from SH-APPΔC cells. The results suggest that cleavage at the Aβ5 site occurs during apoptosis in SH-APP cells.

CONCLUSIONS AND SIGNIFICANCE

Recent evidence suggests that apoptosis underlies the neuronal death seen in AD. Active forms of caspases and the caspase-cleaved APP have been detected in AD brain tissues, but it is not clear whether the caspase cleavage of APP affects Aβ formation. In this study, we have clearly demonstrated that such APP cleavage promotes the secretion of a distinct amino-truncated Aβ species (Aβ5-40/42). Our data provide the first evidentiary connection between caspase activation and the formation of amino-truncated Aβ. Our results are consistent with and expand upon data from previous studies that measured N-terminally intact Aβ, but not amino-truncated Aβ.

We used inhibitors of BACE and α-secretase to investigate the mechanism of Aβ5-40/42 generation. After treatment of SH-APP cells with a BACE inhibitor, OM99-2, Aβ1-40 levels were decreased, whereas Aβ5-40 levels were increased. Treatment of SH-APPΔC cells with TAPI-1 led to decreased Aβ5-40 and increased Aβ1-40 levels. The data strongly suggest that cleavage at the Aβ5 site is not ascribed to BACE1 activity, but mediated by α-secretase-like proteases (e.g., ADAM family proteases, including TACE and ADAM10). This is consistent with the finding that secretion of p3 (Aβ17-40), a product derived from α-secretase cleavage, is significantly increased in cells expressing APPΔC. BACE2 functions as an alternative α-secretase, but may not be involved in Aβ5-40/42 generation, since OM99-2 inhibits BACE1 and BACE2.

It has been established that wild-type APP undergoes caspase cleavage during apoptosis, so it is reasonable to assume that subsequent cleavage at the Aβ5 site occurs in apoptotic cells. We show evidence that APPΔC is generated in SH-APP cells exposed to MG-132 and staurosporine. β'-CTFΔC, which corresponds to a precursor of Aβ5-40/42, is formed in these apoptotic cells. Accordingly, we conclude that Aβ5-40/42 is generated after caspase activation (**Fig. 2**).

Our sensitive Western blot analyses indicate that the majority of intracellular Aβ consist of Aβ1-40/42 in wild-type APP- and APPΔC-expressing cells. Since two distinct pathways appear to exist for extracellular and intracellular pools of Aβ, amino-truncated Aβ peptides, including Aβ5-40/42, are likely to be produced mainly in the extracellular Aβ pathway.

Our immunohistochemical staining with the Aβ5 antibody revealed that Aβ5-40/42 species are deposited in some vessels with amyloid angiopathy in AD brain tissue. This may reflect the in vivo occurrence of caspase cleavage of APP. The observation that Aβ5 antibody labels NFT is intriguing, considering that activation of caspases is suggested to occur in neurons bearing NFT. Our data are consistent with previous reports that considerable N-terminal modifications of Aβ are seen in AD cortices and leptomeninges. Such amino-truncated Aβ species may be instrumental in the amyloidosis process.

We suggest that caspase activation in the AD brain results in the formation of APPΔC, leading to the increased production and deposition of N-terminally truncated Aβ5-40/42. Further research on the in vivo generation of this Aβ species is needed to clarify its pathological role in Aβ deposition and neuronal death in AD. FJ

European Journal of Neuroscience, Vol. 19, pp. 258–264, 2004

Enhanced generation of intracellular Aβ42 amyloid peptide by mutation of presenilins PS1 and PS2

Kazuya Takeda,[1,2] Wataru Araki[1] and Takeshi Tabira[2]
[1]Department of Demyelinating Disease and Ageing, National Institute of Neuroscience, NCNP, 4-1-1 Ogawahigashi, Kodaira, Tokyo, Japan
[2]National Institute for Longevity Sciences, Obu, Aichi, Japan

Keywords: Alzheimer's disease, endosome, neuroblastoma, *trans*-Golgi network

Abstract

The accumulation of amyloid β-peptide (Aβ) in the brain is a critical pathological process in Alzheimer's disease (AD). Recent studies have implicated intracellular Aβ in neurodegeneration in AD. To investigate the generation of intracellular Aβ, we established human neuroblastoma SH-SY5Y cells stably expressing wild-type amyloid precursor protein (APP), Swedish mutant APP, APP plus presenilin 1 (PS1) and presenilin 2 (PS2; wild-type or familial AD-associated mutant), and quantified intracellular Aβ40 and Aβ42 in formic acid extracts by sensitive Western blotting. Levels of both intracellular Aβ40 and Aβ42 were 2–3-fold higher in cells expressing Swedish APP, compared with those expressing wild-type APP. Intracellular Aβ42/Aβ40 ratios were approximately 0.5 in these cells. These ratios were increased markedly in cells expressing mutant PS1 or PS2 compared with those expressing their wild-type counterparts, consistent with the observed changes in secreted Aβ42/Aβ40 ratios. High total levels of intracellular Aβ were observed in cells expressing mutant PS2 because of a marked elevation of Aβ42. Immunofluorescence staining additionally revealed more intense Aβ42 immunoreactivity in mutant PS2-expressing cells than in wild-type cells, which was partially colocalized with immunoreactivity for the *trans*-Golgi network and endosomes. The data collectively indicate that PS mutations promote the accumulation of intracellular Aβ42, which appears to be localized in multiple subcellular compartments.

Introduction

Extracellular senile plaques and intracellular neurofibrillary tangles are the major pathological hallmarks of Alzheimer's disease (AD). Amyloid β-peptide (Aβ) is the main constituent of senile plaques, produced from the proteolytic processing of the amyloid precursor protein (APP) by β- and γ-secretases (Sisodia & St George-Hyslop, 2002). γ-Secretase cleavage of APP results in the generation of short and long forms of Aβ, specifically, Aβ40 and Aβ42. Aβ42 is the minor species in normal metabolism, but is more amyloidogenic and deposited early in the AD brain. The activity of β- and γ-secretase is mediated mainly by BACE (Vassar *et al.*, 1999) and the multimeric presenilin 1 (PS1) complex (De Strooper, 2003), respectively.

The generation of Aβ is known to occur intracellularly. This intracellular pool of Aβ is detectable (Tienari *et al.*, 1997; Morishima-Kawashima & Ihara, 1998; Skovronsky *et al.*, 1998), but precise quantification of this protein is difficult because of its low levels and insoluble nature. Because the amyloid plaque number does not correlate with the degree of dementia and neuronal loss (Neve & Robakis, 1998), intracellular Aβ might play a significant role in the pathogenesis of AD (Echeverria & Cuello, 2002; Tabira *et al.*, 2002a). This view is supported by data from several recent studies. The number of intracellular Aβ42-positive neurons increase significantly in aged mutant PS1 transgenic mice displaying accerelated neurodegeneration (Chui *et al.*, 1999). Intraneuronal Aβ42 deposits detected in AD brains (Gouras *et al.*, 2000) could be associated with apoptotic death (Chui *et al.*, 2001). Moreover, intraneuronal Aβ42 is abundant in younger Down's syndrome brains (Mori *et al.*, 2002), and its accumulation might thus precede Aβ plaque deposition. Intracellular Aβ42 exerts a neurotoxic effect and induces neuronal apoptosis (Kienlen-Campard *et al.*, 2002; Zhang *et al.*, 2002).

Mutations in *PS1* and *PS2* genes are linked to familial AD (Ephrat *et al.*, 1995; Sherrington *et al.*, 1995), and affect the γ-secretase processing of APP to increase Aβ42 secretion (Scheuner *et al.*, 1996; Citron *et al.*, 1997). Recent evidence suggests that both PS1 and PS2 mediate γ-secretase activity, although the PS1-containing complex is more active than that containing PS2 (Lai *et al.*, 2003). An unusual form of senile plaque (cotton wool-type plaques) develop in some cases of familial AD with PS1 mutations. In these plaques, Aβ42 appears to be deposited in synaptic structures (Tabira *et al.*, 2002b).

In the present study, we developed a method to measure the amount of intracellular Aβ semiquantitatively and analyse the effects of the PS mutations on intracellular Aβ in human neuronal cells. We additionally performed immunocytochemical analysis of intracellular Aβ42 to determine its subcellular localization.

Materials and methods

Antibodies

A monoclonal antibody to APP was obtained from Roche Diagnostics (Mannheim, Germany). Polyclonal antibodies to PS1 (Ab111) and PS2 (Ab333) were generated and purified as described previously (Chui *et al.*, 1998; Shirotani *et al.*, 1999). Three Aβ-specific monoclonal antibodies were used: BA27 (specific for Aβ40); BC05 (specific for Aβ42); and BNT77 (specific for Aβ11–28; the epitope comprises

Correspondence: Dr W. Araki, as above.
E-mail: araki@ncnp.go.jp

Received 8 August 2003, revised 8 October 2003, accepted 5 November 2003

doi:10.1111/j.1460-9568.2003.03135.x

Aβ11–16; gifts from Takeda Chemical Industries., Osaka, Japan) (Suzuki *et al.*, 1994; Asami-Odaka *et al.*, 1995). Polyclonal antibodies to calnexin, γ1-adaptin and early endosomal antigen 1 (EEA1) were purchased from Chemicon (Temecula, CA, USA), Santa Cruz Biotechnology (Santa Cruz, CA, USA) and Affinity Bioreagents (Golden, CO, USA), respectively.

Cell culture and transfection

Human neuroblastoma SH-SY5Y cells were maintained in a humidified atmosphere of 5% CO_2/95% air in DMEM/F12 medium containing 10% fetal bovine serum. Human wild-type *APP695* (*APP*) or Swedish mutant *APP695* (*swAPP*) cDNA was introduced into the *EcoR*V site of pcDNA3.1 expression vector (Invitrogen, Carlsbad, CA). Human wild-type or mutant (G384A) *PS1* cDNA and wild-type or mutant (N141I) *PS2* cDNA were subcloned into the pCEP4 vector (Invitrogen) as described previously (Shirotani *et al.*, 1999). SH-SY5Y cells were transfected with APP or swAPP using the calcium phosphate method, and clones were selected with G418 for stable integration. A SH-SY5Y cell clone stably expressing high levels of APP was established, followed by transfection with PS1 or PS2 (wild-type or mutant). Clones expressing APP + PS1 or PS2 (wild-type or mutant) were selected with hygromycin.

Immunoblotting

Immunoblot analyses were performed as described previously (Araki *et al.*, 2001). Cells were lysed in RIPA buffer [10 mM Tris, pH 8.0, 150 mM NaCl, 1% NP-40, 0.5% sodium deoxycholate, 0.1% sodium dodecylsulphate (SDS), 5 mM EDTA] containing protease inhibitors. Proteins were separated on 12% polyacrylamide gels and blotted onto PVDF membranes. Blots were blocked in phosphate-buffered saline (PBS) containing 0.05% Tween-20 and 5% nonfat dry milk, and probed with anti-APP, anti-PS1 or anti-PS2 antibodies. Membranes were subsequently incubated with secondary peroxidase-labelled anti-rabbit or anti-mouse IgG, and protein expression was detected with chemiluminescence reagents (Dupont NEN, Boston, MA, USA).

Semiquantitative analysis of intracellular Aβ

Cells were washed with ice-cold PBS and harvested using a scraper. Cell pellets were homogenized in ice-cold Tris-buffered saline (pH 8.0) containing protease inhibitors, and postnuclear fractions were collected as supernatants after centrifugation at 600 *g* for 10 min at 4 °C. Samples containing 400 μg protein were further centrifuged at 100 000 *g* for 1 h in a TLX ultracentrifuge (Beckman, Fullerton, CA, USA). Because the Aβ concentration in the supernatant fractions was much lower than that in pellets (data not shown), only the latter membrane fractions were used for analysis. Pellets were washed with chloroform/methanol [2 : 1 (v/v)], sonicated in 70% formic acid, and incubated at 4 °C overnight, followed by drying in a centrifugal concentrator. Samples and standard Aβ peptides were solubilized in Tris-Tricine SDS sample buffer containing 7.8 M urea and subjected to Tris-Tricine SDS-polyacrylamide gel electrophoresis. Separated proteins were transferred to a nitrocellulose membrane (Schleicher and Schuell, Germany), and reacted with BA27 or BC05 antibodies after boiling (Ida *et al.*, 1996). Aβ40 and Aβ42 levels in samples were semiquantified by comparing band intensities with those of the synthetic Aβ1–40 and Aβ1–42 peptide (Bachem, Budendorf, Switzerland) standards, respectively, using an image analyser LAS-1000 (Fuji Film Co., Japan).

Enzyme-linked immunosorbent assay (ELISA)

The levels of Aβ40 and Aβ42 in conditioned medium were measured using sandwich ELISA, as described previously (Suzuki *et al.*, 1994; Asami-Odaka *et al.*, 1995). BNT77 was coated as a capture antibody on a 96-well plate. Samples (0.1 mL) and standard peptides, Aβ1–40 or Aβ1–42, were applied to a BNT77-coated plate and incubated at 4 °C overnight. After rinsing with PBS, the plate was reacted with horseradish peroxidase-conjugated BA27 or BC05 at 4 °C overnight. Bound-enzyme activity was measured using the TMB Microwell Peroxidase Substrate System (Kirkegaard & Perry Laboratory, Gaithersburg, MD, USA).

Immunocytochemistry

Stably transfected SH-SY5Y cells were cultured on slides (Becton Dickinson, NJ, USA), and fixed in 2% paraformaldehyde and 0.2% glutaraldehyde in PBS for 15 min at room temperature. Fixed cells were permeabilized with 0.3% Triton X-100 in PBS, incubated with anti-Aβ42 (BC05) or anti-Aβ40 (BA27) antibody for 1 h and fluorescein isothiocyanate (FITC)-conjugated anti-mouse IgG for 1 h. For double immunolabelling, cells were subsequently stained with anti-calnexin, anti-γ1-adaptin or anti-EEA1 antibody and rhodamine-conjugated anti-rabbit IgG. Specimens were examined with a confocal laser scanning microscope imaging system (Olympus FLUOVIEW).

Results

To investigate the generation of intracellular Aβ, we initially established stable SH-SH5Y clones expressing APP and swAPP (designated

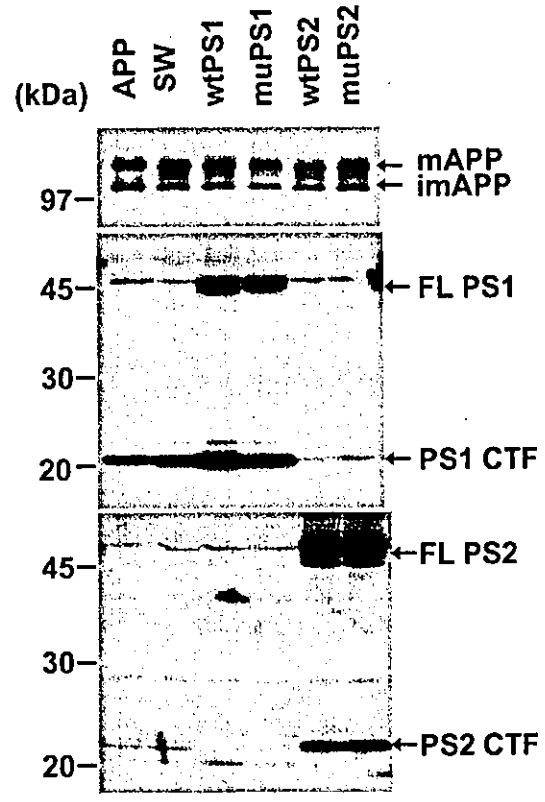

FIG. 1. Expression of APP, PS1 and PS2 in stably transfected SH-SY5Y cells. Cell lysates from SH-APP (APP), SH-swAPP (SW), SH-APP + wtPS1 (wtPS1), SH-APP + muPS1 (muPS1), SH-APP + wtPS2 (wtPS2), SH-APP + muPS2 (muPS2) were subjected to Western blotting with anti-APP, anti-PS1, and anti-PS2 antibodies. The levels of mature and immature APP (mAPP and imAPP) were almost equivalent in these cell lines. PS1 and PS2 expression levels were similar between SH-APP + wtPS1 and SH-APP + muPS1 and between SH-APP + wtPS2 and SH-APP + muPS2, respectively. Levels of endogenous PS1 and PS2 C-terminal fragments (CTF) were reduced in PS2-expressing and PS1-expressing cells, respectively, as a result of the replacement effect (Thinakaran *et al.*, 1996). FL, full-length.

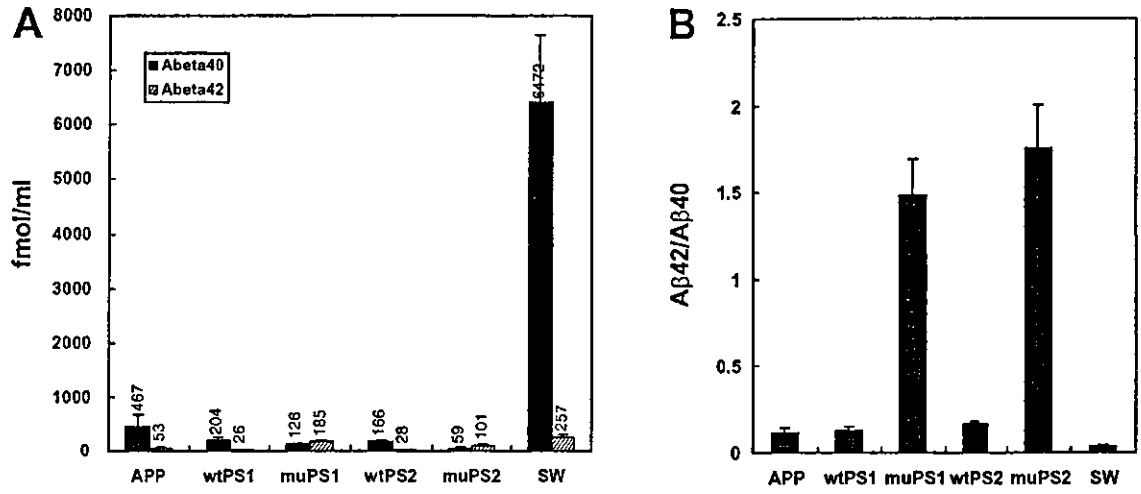

FIG. 2. ELISA analysis of secreted Aβ from stably transfected SH-SY5Y cells. (A) Indicated cell lines were cultured on a 12-well plate, and levels of Aβ40 and Aβ42 in 24 h-conditioned medium were quantified by sandwich ELISA, as described in Materials and methods. (B) Ratios of secreted Aβ42/Aβ40. Ratios were increased markedly in SH-APP + muPS1 and SH-APP + muPS2 cells, compared with other cell lines. In both graphs, values represent means ± SD of data from four independent experiments.

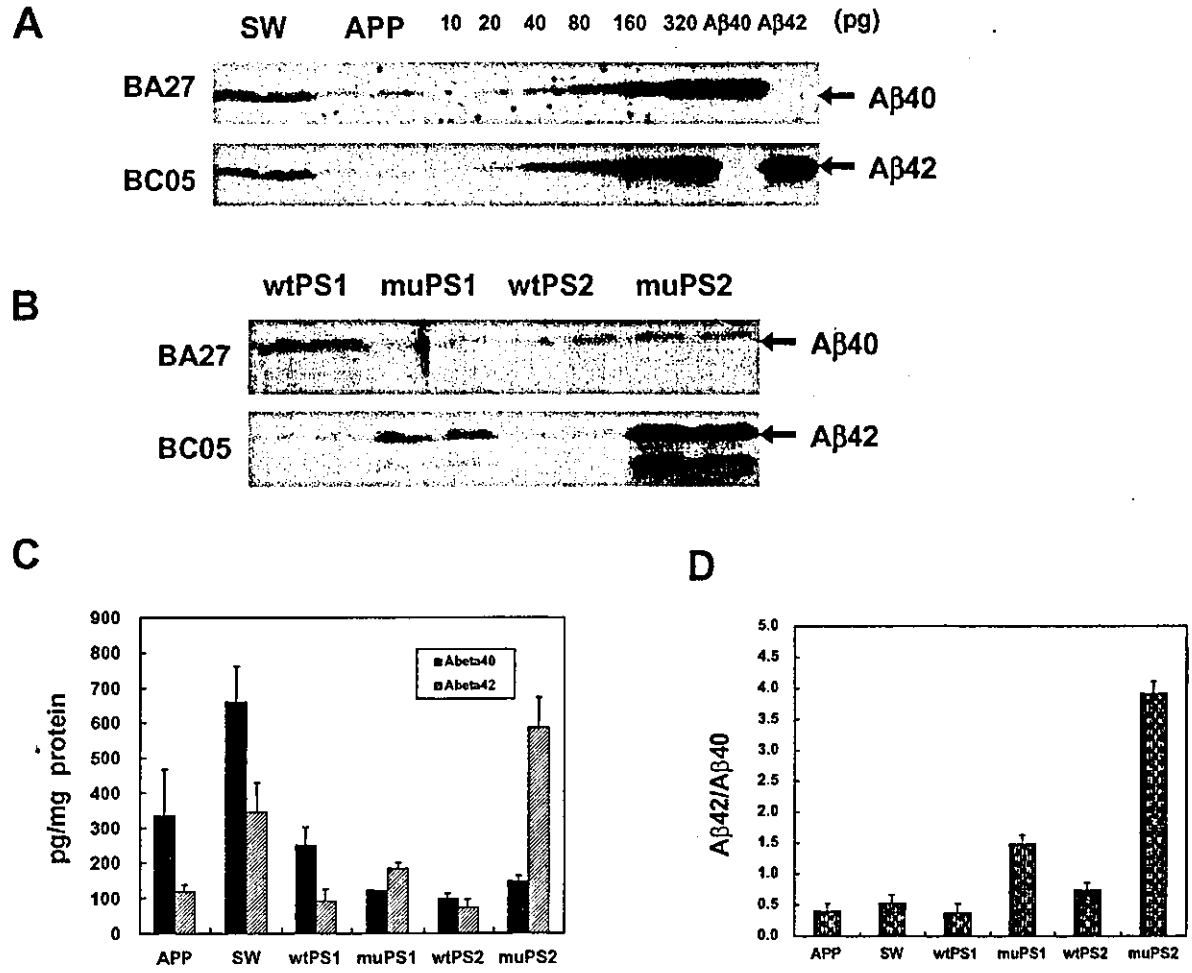

FIG. 3. Semiquantitative analysis of intracellular Aβ40 and Aβ42. (A) Formic acid extracts from total membrane fractions of SH-APP, SH-swAPP and standard synthetic Aβ40 and Aβ42 were subjected to Western blot analysis with BA27 or BC05, as described in Materials and methods. Both intracellular Aβ40 and Aβ42 levels were increased significantly in SH-swAPP cells, compared with SH-APP cells. (B) Intracellular Aβ40 and Aβ42 levels in SH-APP + wtPS1, SH-APP + muPS1, SH-APP + wtPS2 and SH-APP + muPS2 cells were analysed as in A. Intracellular Aβ42 levels were higher in mutant than wild-type PS-expressing cells. (C and D) Graphs showing estimated levels of intracellular Aβ40 and Aβ42 (C) and ratios of intracellular Aβ42/Aβ40 (D). Intracellular Aβ42/Aβ40 ratios were significantly higher in SH-APP + muPS1 and SH-APP + muPS2 cells, compared with other cell lines. In both graphs, the values represent means ± SD of data from three independent experiments.

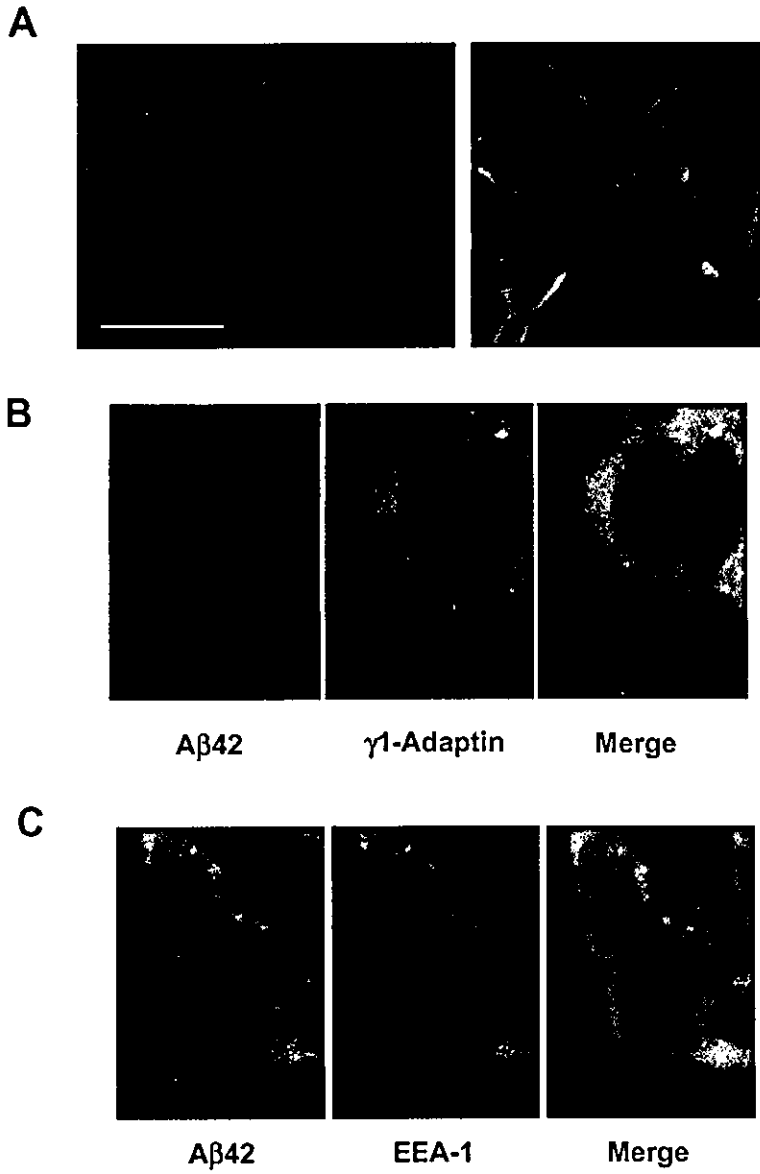

FIG. 4. Immunocytochemical analysis of intracellular Aβ42. (A) SH-APP + wtPS2 (left) and SH-APP + muPS2 (right) cells were stained with BC05 antibody. Aβ42 was visualized with FITC-conjugated anti-mouse IgG. Immunoreactivity was more intense in SH-APP + muPS2 cells, compared to SH-APP + wtPS2 cells. Scale bar, 50 μm. (B) Double immunofluorescence staining with anti-Aβ42 and anti-γ1-adaptin. SH-APP + muPS2 cells were double-immunolabelled with BC05 and anti-γ1-adaptin. γ1-Adaptin was visualized with rhodamine-conjugated anti-rabbit IgG. The merged image signifies partial colocalization of immunoreactivities for Aβ42 and γ1-adaptin. (C) Double immunofluorescence staining with anti-Aβ42 and anti-EAA1. SH-APP + muPS2 cells were double-immunolabelled as in B. The merged image depicts partial colocalization of immunoreactivities for Aβ42 and EEA1.

SH-APP and SH-swAPP). The former clone was employed as the parental cell line for generating stable clones coexpressing APP and PS1 (wild-type or G384A mutant; designated SH-APP + wtPS1 and SH-APP + muPS1) as well as APP and PS2 (wild-type or N141I mutant; designated SH-APP + wtPS2 and SH-APP + muPS2). These six clones expressed almost equivalent levels of APP and grew normally. Expression levels of PS1 were similar in SH-APP + wtPS1 and SH-APP + muPS1 cells, and expression levels of PS2 were equivalent between SH-APP + wtPS2 and SH-APP + muPS2 cells (Fig. 1).

Levels of secreted Aβ in stable transfectants were examined by sandwich ELISA. SH-swAPP cells secreted ~14-fold and ~5-fold higher levels of Aβ40 and Aβ42 than SH-APP cells, respectively. Reduced Aβ40 and increased Aβ42 secretion was observed in SH-APP + muPS1 and SH-APP + muPS2 cells, compared with SH-APP + wtPS1 and SH-APP + wtPS2 cells (Fig. 2A). Mutant PS-expressing clones exhibited significantly higher secreted Aβ42/Aβ40 ratios than wild-type PS-expressing clones (Fig. 2B), confirming enhanced Aβ42 secretion by mutations in PS.

Next, we analysed the levels of intracellular Aβ by sensitive Western blotting. The membrane fraction containing intracellular Aβ was delipidated with chloroform and methanol and solubilized with formic acid. Extracted protein samples and synthetic Aβ standards were subjected to Western blotting with BA27 (specific for Aβ40) or BC05 (specific for Aβ42) antibodies. Levels of intracellular Aβ40 and Aβ42 in SH-swAPP cells were ~2-fold and ~3-fold higher, respectively, than those in SH-APP cells (Fig. 3A and C). Intracellular Aβ42/Aβ40 ratios were 0.4–0.5 in these cell lines (Fig. 3D). We examined the effects of PS1 and PS2 mutations on intracellular Aβ generation. Aβ40 was decreased and Aβ42 was increased in

SH-APP + muPS1 cells, compared with SH-APP + wtPS1 cells (Fig. 3B and C). Consequently, the intracellular Aβ42/Aβ40 ratio was much higher in the former cell line (Fig. 3D). Levels of Aβ40 were not significantly altered, whereas Aβ42 increased remarkably in SH-APP + muPS2 cells, compared with SH-APP + wtPS2 cells. The former cell line exhibited a marked increase in the intracellular Aβ42/Aβ40 ratio (Fig. 3B–D). Interestingly, total levels of intracellular Aβ (Aβ40 + Aβ42) were additionally elevated significantly in SH-APP + muPS2 cells. The data conclusively establish that generation of intracellular Aβ42 is enhanced by PS mutations.

We next investigated whether the increased intracellular Aβ42 induced by PS mutations could be detected immunocytochemically. To address this issue, we used SH-APP + wtPS2 and SH-APP + muPS2 cells, because of the marked difference in the intracellular Aβ42 levels in these cell lines. Immunofluorescence staining of cells with BC05 revealed that the intensity of BC05-positive immunoreactivity was higher in SH-APP + muPS2 cells than SH-APP + wtPS2 cells, although the mesh-like staining pattern was similar in both cells (Fig. 4A). In contrast, BA27 staining intensity was similar in both cells (data not shown).

To determine the subcellular localization of intracellular Aβ42, we performed double immunofluorescence staining using antibodies to γ1-adaptin [a marker for the *trans*-Golgi network (TGN)], calnexin [a marker for endoplasmic reticulum (ER)], and EEA1 (a marker for endosomes). The specificities of these antibodies were confirmed by Western blotting of cell lysates (data not shown). When SH-APP + muPS2 cells were double-stained with BC05 and anti-γ1-adaptin, positive stains partially overlapped (Fig. 4B). BC05 immunoreactivity was not clearly colocalized with that of anti-calnexin (data not shown). In addition, positive staining for anti-EAA1 was colocalized partially with that of BC05 (Fig. 4C). Double immunostaining of SH-APP + wtPS2 cells showed similar colocalization of BC05 immunoreactivity with that of anti-γ1-adaptin and anti-EEA1 (data not shown). The data suggest that intracellular Aβ42 is localized in multiple compartments, including TGN and endosomes. No difference in intracellular Aβ42 localization was seen between mutant PS2- and wild-type PS2-expressing cells.

Discussion

We have established a reliable method to measure intracellular Aβ40 and Aβ42 levels semiquantitatively, using sensitive Western blotting with highly specific antibodies. This method facilitates analysis of the effects of Swedish APP and PS mutations on intracellular Aβ in human neuronal cells. Intracellular Aβ40 and Aβ42 levels were higher in SH-swAPP than SH-APP cells, but the intracellular Aβ42/Aβ40 ratios were similar (~0.5) in both cell lines. This ratio is higher than that of secreted Aβ42/Aβ40, suggesting that Aβ42 constitutes the larger fraction in the intracellular compared with the secreted pool. A previous study using immunoprecipitation-Western blotting estimated an intracellular Aβ42/Aβ40 ratio of ~0.2 in primary neurons (Tienari *et al.*, 1997). However, using an ELISA system, Skovronsky *et al.* (1998) reported an intracellular Aβ42/Aβ40 ratio of ~1.5 in NT2N neurons. It remains unclear whether the discrepancies between the data are a result of differences in quantification methods or cell types.

Intracellular Aβ42/Aβ40 ratios were increased significantly in cells expressing mutant PS1 or PS2, compared with those expressing the wild-type counterparts. Our results confirm that PS mutations exert an Aβ42-promoting effect, both intra- and extracellularly (Petanceska *et al.*, 2000; Iwata *et al.*, 2001). Interestingly, total levels of intracellular Aβ in SH-APP + muPS2 cells were much higher than those in SH-APP + wtPS2 cells, because of the marked elevation in intracellular Aβ42. The reasons for the significant effect of mutations in PS2 on intracellular Aβ42 are currently unclear, but could be related to the relatively inefficient secretion of Aβ42.

The p3 fragment derived from α-secretase cleavage was hardly detectable on Western blots of intracellular Aβ, suggesting that the majority of intracellular Aβ consists of Aβ1–40/42. As two distinct pathways appear to exist for extracellular and intracellular pools of Aβ, p3 is possibly produced mainly in the extracellular Aβ pathway (Tienari *et al.*, 1997).

The subcellular sites at which Aβ40 and Aβ42 are generated are yet to be established. Some previous studies favour the TGN as the major site of Aβ generation (Greenfield *et al.*, 1999; Petanceska *et al.*, 2000; Sudoh *et al.*, 2000; Iwata *et al.*, 2001; Siman & Velji, 2003). Other investigators suggest that Aβ42, but not Aβ40, is produced in ER (Cook *et al.*, 1997; Hartmann *et al.*, 1997). The endosomal pathway additionally contributes significantly to Aβ generation (Perez *et al.*, 1999; Grbovic *et al.*, 2003). It should be noted that immunocytochemical staining with Aβ antibodies is not useful in identifying the Aβ generation sites, but provides information on subcellular localization. Our immunocytochemical data confirm enhanced generation of intracellular Aβ42 in cells expressing mutant PS2, and suggest distribution in both secretory (TGN) and endocytic (endosome) compartments. The results are consistent with the previous finding that Aβ immunoreactivity is localized to several intracellular compartments in neuronally differentiated embryonal carcinoma cells (Grant *et al.*, 2000) and human astrocytes from Down's syndrome brains (Busciglio *et al.*, 2002). A recent ultrastructural study additionally demonstrated that Aβ42 is localized to multivesicular bodies which are part of the lysosomal/endosomal system (Takahashi *et al.*, 2002). However, our finding is not consistent with recent data showing a distinct intracellular pool of Aβ42 in an ER/intermediate compartment (Cook *et al.*, 1997; Wilson *et al.*, 2002). This discrepancy could be because of differences in the cell types used.

Intraneuronal Aβ deposits are observed more abundantly in brains of transgenic mice expressing both APP and mutant PS1 at early stages. (Wirths *et al.*, 2001, 2002). Similarly, intraneuronal Aβ42 immunoreactivity is more abundant in younger Down's syndrome brains (Mori *et al.*, 2002). Furthermore, the appearance of physiological and behavioural abnormalities precedes amyloid plaque deposition in some transgenic mouse models of AD (Hsia *et al.*, 1999; Moechars *et al.*, 1999). These data support the view that intraneuronal accumulation of Aβ42 occurs before extracellular deposition and is relevant to neuronal dysfunction. Lowering intracellular Aβ42 levels is an important consideration in the design of therapeutic approaches for AD. Further research to clarify the role of intracellular Aβ in AD pathogenesis should facilitate the development of effective treatment regimes for AD.

Acknowledgements

We thank Takeda Chemical Industries Ltd. for Aβ antibodies, Masayoshi Sawada for technical assistance and Drs Maho Morishima-Kawashima and Yasuo Ihara for helpful suggestions. This work was partially supported by grants from the Ministry of Health, Labour and Welfare and Grant-in-Aid for Scientific Research on Priority Areas from the Ministry of Education, Science, Sports and Culture in Japan.

Abbreviations

AD, Alzheimer's disease; Aβ, amyloid β-peptide; APP, amyloid precursor protein; PS1, presenilin 1; PS2, presenilin 2; EEA1, early endosomal antigen 1; ELISA, enzyme-linked immunosorbent assay; ER, endoplasmic reticulum; FITC, fluorescein isothiocyanate; TGN, *trans*-Golgi network.

References

Araki, W., Yuasa, K., Takeda, S., Takeda, K., Shirotani, K., Takahashi, K. & Tabira, T. (2001) Pro-apopototic effect of presenilin 2 (PS2) overexpression is associated with downregulation of Bcl-2 in cultured neurons. *J. Neurochem.*, **79**, 1161–1168.

Asami-Odaka, A., Ishibashi, Y., Kikuchi, T., Kitada, C. & Suzuki, N. (1995) Long amyloid beta-protein secreted from wild-type human neuroblastoma IMR-32 cells. *Biochemistry*, **34**, 10272–10278.

Busciglio, J., Pelsman, A., Wong, C., Pigino, G., Yuan, M., Mori, H. & Yankner, B.A. (2002) Altered metabolism of the amyloid beta precursor protein is associated with mitochondrial dysfunction in Down's syndrome. *Neuron*, **33**, 677–688.

Chui, D.H., Dobo, E., Makifuchi, T., Akiyama, H., Kawakatsu, S., Petit, A., Checler, F., Araki, W., Takahashi, K. & Tabira, T. (2001) Apopototic neurons in Alzheimer's Disease frequently show intracellular Abeta42 labeling. *J. Alzheimer's Dis.*, **3**, 231–239.

Chui, D.H., Shirotani, K., Tanahashi, H., Akiyama, H., Ozawa, K., Kunishita, T., Takahashi, K., Makifuchi, T. & Tabira, T. (1998) Both N-terminal and C-terminal fragments of presenilin 1 colocalize with neurofibrillary tangles in neurons and dystrophic neurites of senile plaques in Alzheimer's disease. *J. Neurosci. Res.*, **53**, 99–106.

Chui, D.H., Tanahashi, H., Ozawa, K., Ikeda, S., Checler, F., Ueda, O., Suzuki, H., Araki, W., Inoue, H., Shirotani, K., Takahashi, K., Gallyas, F. & Tabira, T. (1999) Transgenic mice with Alzheimer presenilin 1 mutations show accelerated neurodegeneration without amyloid plaque formation. *Nat. Med.*, **5**, 560–564.

Citron, M., Westaway, D., Xia, W., Carlson, G., Diehl, T., Levesque, G., Johnson-Wood, K., Lee, M., Seubert, P., Davis, A., Kholodenko, D., Motter, R., Sherrington, R., Perry, B., Yao, H., Strome, R., Lieberburg, I., Rommens, J., Kim, S., Schenk, D., Fraser, P., St George-Hyslop, P. & Selkoe, D.J. (1997) Mutant presenilins of Alzheimer's disease increase production of 42-residue amyloid beta-protein in both transfected cells and transgenic mice. *Nat. Med.*, **3**, 67–72.

Cook, D.G., Forman, M.S., Sung, J.C., Leight, S., Kolson, D.L., Iwatsubo, T., Lee, V.M. & Doms, R.W. (1997) Alzheimer's Abeta (1–42) is generated in the endoplasmic reticulum/intermediate compartment of NT2N cells. *Nat. Med.*, **3**, 1021–1023.

De Strooper, B. (2003) Aph-1, Pen-2, and Nicastrin with Presenilin generate an active gamma-secretase complex. *Neuron*, **38**, 9–12.

Echeverria, V. & Cuello, A.C. (2002) Intracellular A-beta amyloid, a sign for worse things to come? *Mol. Neurobiol.*, **26**, 299–316.

Ephrat, L.-L., Wasco, W., Poorkaj, P., Romano, D.M., Oshima, J. & Pettingell, W.H., YuC.-E., Jondro, P.D., Schmidt, S.D., Wang, K., Crowley, A.C., Fu, Y.-H., Guenette, S.Y., Galas, D., Nemens, E., Wijsman, E.M., Bird, T.D., Schellenberg, G.D. & Tanzi, R.E. (1995) Candidate gene for the chromosome 1 familial Alzheimer's disease locus. *Science*, **269**, 973–977.

Gouras, G.K., Tsai, J., Naslund, J., Vincent, B., Edgar, M., Checler, F., Greenfield, J.P., Haroutunian, V., Buxbaum, J.D., Xu, H., Greengard, P. & Relkin, N.R. (2000) Intraneuronal Aβ42 accumulation in human brain. *Am. J. Pathol.*, **156**, 15–20.

Grant, S.M., Ducatenzeiler, A., Szyf, M. & Cuello, A.C. (2000) Aβ immunoreactive material is present in several intracellular compartments in transfected, neuronally differentiated, P19 cells expressing the human amyloid beta-protein precursor. *J. Alzheimer's Dis.*, **2**, 207–222.

Grbovic, O.M., Mathews, P.M., Jiang, Y., Schmidt, S.D., Dinakar, R., Summers-Terio, N.B., Ceresa, B.P., Nixon, R.A. & Cataldo, A.M. (2003) Rab5-stimulated up-regulation of the endocytic pathway increases intracellular levels of betaCTFs and Abeta production. *J. Biol. Chem.*, **278**, 31261–31268.

Greenfield, J.P., Tsai, J., Gouras, G.K., Hai, B., Thinakaran, G., Checler, F., Sisodia, S.S., Greengard, P. & Xu, H. (1999) Endoplasmic reticulum and trans-Golgi network generate distinct populations of Alzheimer beta-amyloid peptides. *Proc. Natl. Acad. Sci. USA*, **96**, 742–747.

Hartmann, T., Bieger, S.C., Bruhl, B., Tienari, P.J., Ida, N., Allsop, D., Roberts, G.W., Masters, C.L., Dotti, C.G., Unsicker, K. & Beyreuther, K. (1997) Distinct sites of intracellular production for Alzheimer's disease A beta40/42 amyloid peptides. *Nat. Med.*, **3**, 1016–1020.

Hsia, A.Y., Masliah, E. & McConlogue, L., YuG.Q., Tatsuno, G., Hu, K., Kholodenko, D., Malenka, R.C., Nicoll, R.A. & Mucke, L. (1999) Plaque-independent disruption of neural circuits in Alzheimer's disease mouse models. *Proc. Natl. Acad. Sci. USA*, **96**, 3228–3233.

Ida, N., Hartmann, T., Pantel, J., Schroder, J., Zerfass, R., Forstl, H., Sandbrink, R., Masters, C.L. & Beyreuther, K. (1996) Analysis of heterogeneous A4 peptides in human cerebrospinal fluid and blood by a newly developed sensitive Western blot assay. *J. Biol. Chem.*, **271**, 22908–22914.

Iwata, H., Tomita, T., Maruyama, K. & Iwatsubo, T. (2001) Subcellular compartment and molecular subdomain of beta-amyloid precursor protein relevant to the Abeta 42-promoting effects of Alzheimer mutant presenilin 2. *J. Biol. Chem.*, **276**, 21678–21685.

Kienlen-Campard, P., Miolet, S., Tasiaux, B. & Octave, J.N. (2002) Intracellular amyloid-beta 1–42, but not extracellular soluble amyloid-beta peptides, induces neuronal apoptosis. *J. Biol. Chem.*, **277**, 15666–15670.

Lai, M.T., Chen, E., Crouthamel, M.C., DiMuzio-Mower, J., Xu, M., Huang, Q., Price, E., Register, R.B., Shi, X.P., Donoviel, D.B., Bernstein, A., Hazuda, D., Gardell, S.J. & Li, Y.M. (2003) Presenilin-1 and presenilin-2 exhibit distinct yet overlapping gamma-secretase activities. *J. Biol. Chem.*, **278**, 22475–22481.

Moechars, D., Dewachter, I., Lorent, K., Reverse, D., Baekelandt, V., Naidu, A., Tesseur, I., Spittaels, K., Haute, C.V., Checler, F., Godaux, E., Cordell, B. & Van Leuven, F. (1999) Early phenotypic changes in transgenic mice that overexpress different mutants of amyloid precursor protein in brain. *J. Biol. Chem.*, **274**, 6483–6492.

Mori, C., Spooner, E.T., Wisniewsk, K.E., Wisniewski, T.M., Yamaguch, H., Saido, T.C., Tolan, D.R., Selkoe, D.J. & Lemere, C.A. (2002) Intraneuronal Abeta42 accumulation in Down syndrome brain. *Amyloid*, **9**, 88–102.

Morishima-Kawashima, M. & Ihara, Y. (1998) The presence of amyloid beta-protein in the detergent-insoluble membrane compartment of human neuroblastoma cells. *Biochemistry*, **37**, 15247–15253.

Neve, R.I. & Robakis, N.K. (1998) Alzheimer's disease: a re-examination of the amyloid hypothesis. *Trends Neurosci.*, **21**, 15–19.

Perez, R.G., Soriano, S., Hayes, J.D., Ostaszewski, B., Xia, W., Selkoe, D.J., Chen, X., Stokin, G.B. & Koo, E.H. (1999) Mutagenesis identifies new signals for beta-amyloid precursor protein endocytosis, turnover, and the generation of secreted fragments, including Abeta42. *J. Biol. Chem.*, **274**, 18851–18856.

Petanceska, S.S., Seeger, M., Checler, F. & Gandy, S. (2000) Mutant presenilin 1 increases the levels of Alzheimer amyloid beta-peptide Abeta42 in late compartments of the constitutive secretory pathway. *J. Neurochem.*, **74**, 1878–1884.

Scheuner, D., Eckman, C., Jensen, M., Song, X., Citron, M., Suzuki, N., Bird, T.D., Hardy, J., Hutton, M., Kukull, W., Larson, E., Levy-Lahad, E., Viitanen, M., Peskind, E., Poorkaj, P., Schellenberg, G., Tanzi, R., Wasco, W., Lannfelt, L., Selkoe, D. & Younkin, S. (1996) Secreted amyloid beta-protein similar to that in the senile plaques of Alzheimer's disease is increased in vivo by the presenilin 1 and 2 and APP mutations linked to familial Alzheimer's disease. *Nat. Med.*, **2**, 864–870.

Sherrington, R., Rogaev, E.I., Liang, Y., Rogaeva, E.A., Levesque, G., Ikeda, M., Chi, H., Lin, C., Li, G., Holman, K., Tsuda, T., Mar, L., Foncin, J.-F., Bruni, A.C., Montesi, M.P., Sorbi, S., Rainero, I., Pinessi, L., Ne, L., Chumakov, I., Pollen, D., Brookes, A., Sanseau, P., Polinsky, R.J., Wasco, W., Dasilva, H.A., Haines, J.L., Pericak-Vance, M.A., Tanzi, R.E., Roses, A.D., Fraser, P.E., Rommens, J.M. & St George-Hyslop, P.H. (1995) Cloning of a gene bearing missense mutations in early-onset familial Alzheimer's disease. *Nature*, **375**, 754–760.

Shirotani, K., Takahashi, K. & Tabira, T. (1999) Effects of presenilin N-terminal fragments on production of amyloid beta peptide and accumulation of endogenous presenilins. *Neurosci. Lett.*, **262**, 37–40.

Siman, R. & Velji, J. (2003) Localization of presenilin-nicastrin complexes and gamma-secretase activity to the trans-Golgi network. *J. Neurochem.*, **84**, 1143–1153.

Sisodia, S.S. & St George-Hyslop, P.H. (2002) gamma-Secretase, Notch, Abeta and Alzheimer's disease: where do the presenilins fit in? *Nat. Rev. Neurosci.*, **3**, 281–290.

Skovronsky, D.M., Doms, R.W. & Lee, V.M. (1998) Detection of a novel intraneuronal pool of insoluble amyloid beta protein that accumulates with time in culture. *J. Cell Biol.*, **141**, 1031–1039.

Sudoh, S., Hua, G., Kawamura, Y., Maruyama, K., Komano, H. & Yanagisawa, K. (2000) Intracellular site of gamma-secretase cleavage for Abeta42 generation in neuro 2a cells harbouring a presenilin 1 mutation. *Eur. J. Biochem.*, **267**, 2036–2045.

Suzuki, N., Cheung, T.T., Cai, X.D., Odaka, A., Otvos, L. Jr, Eckman, C., Golde, T.E. & Younkin, S.G. (1994) An increased percentage of long amyloid beta protein secreted by familial amyloid beta protein precursor (beta APP717) mutants. *Science*, **264**, 1336–1340.

Tabira, T., Chui, D.H. & Kuroda, S. (2002a) Significance of intracellular Abeta42 accumulation in Alzheimer's disease. *Front. Biosci.*, **7**, a44–49.

Tabira, T., Chui, D.H., Nakayama, H., Kuroda, S. & Shibuya, M. (2002b) Alzheimer's disease with spastic paresis and cotton wool type plaques. *J. Neurosci. Res.*, **70**, 367–372.

Takahashi, R.H., Milner, T.A., Li, F., Nam, E.E., Edgar, M.A., Yamaguchi, H., Beal, M.F., Xu, H., Greengard, P. & Gouras, G.K. (2002) Intraneuronal Alzheimer abeta42 accumulates in multivesicular bodies and is associated with synaptic pathology. *Am. J. Pathol.*, **161**, 1869–1879.

Thinakaran, G., Borchelt, D.R., Lee, M.K., Slunt, H.H., Spitzer, L., Kim, G., Ratovitsky, T., Davenport, F., Nordstedt, C., Seeger, M., Hardy, J., Levey, A.I., Gandy, S.E., Jenkins, N.A., Copeland, N.G., Price, D.L. & Sisodia, S.S. (1996) Endoproteolysis of presenilin 1 and accumulation of processed derivatives in vivo. *Neuron*, **17**, 181–190.

Tienari, P.J., Ida, N., Ikonen, E., Simons, M., Weidemann, A., Multhaup, G., Masters, C.L., Dotti, C.G. & Beyreuther, K. (1997) Intracellular and secreted Alzheimer beta-amyloid species are generated by distinct mechanisms in cultured hippocampal neurons. *Proc. Natl. Acad. Sci. USA*, **94**, 4125–4130.

Vassar, R., Bennett, B.D., Babu-Khan, S., Kahn, S., Mendiaz, E.A., Denis, P., Teplow, D.B., Ross, S., Amarante, P., Loeloff, R., Luo, Y., Fisher, S., Fuller, J., Edenson, S., Lile, J., Jarosinski, M.A., Biere, A.L., Curran, E., Burgess, T., Louis, J.C., Collins, F., Treanor, J., Rogers, G. & Citron, M. (1999) Beta-secretase cleavage of Alzheimer's amyloid precursor protein by the transmembrane aspartic protease BACE. *Science*, **286**, 735–741.

Wilson, C.A., Doms, R.W., Zheng, H. & Lee, V.M. (2002) Presenilins are not required for Abeta 42 production in the early secretory pathway. *Nat. Neurosci.*, **5**, 849–855.

Wirths, O., Multhaup, G., Czech, C., Blanchard, V., Moussaoui, S., Tremp, G., Pradier, L., Beyreuther, K. & Bayer, T.A. (2001) Intraneuronal Abeta accumulation precedes plaque formation in beta-amyloid precursor protein and presenilin-1 double-transgenic mice. *Neurosci. Lett.*, **306**, 116–120.

Wirths, O., Multhaup, G., Czech, C., Feldmann, N., Blanchard, V., Tremp, G., Beyreuther, K., Pradier, L. & Bayer, T.A. (2002) Intraneuronal APP/A beta trafficking and plaque formation in beta-amyloid precursor protein and presenilin-1 transgenic mice. *Brain Pathol.*, **12**, 275–286.

Zhang, Y., McLaughlin, R., Goodyer, C. & LeBlanc, A. (2002) Selective cytotoxicity of intracellular amyloid beta peptide1–42 through p53 and Bax in cultured primary human neurons. *J. Cell Biol.*, **156**, 519–529.

The FASEB Journal express article 10.1096/fj.03-1040fje. Published online April 14, 2004.

Glypican-1 as an Aβ binding HSPG in the human brain: Its localization in DIG domains and possible roles in the pathogenesis of Alzheimer's disease

Norifumi Watanabe,* Wataru Araki,† De-Hua Chui,‡ Takao Makifuchi,§ Yasuo Ihara,¶ and Takeshi Tabira*

*National Institute for Longevity Sciences, 36-3 Gengo, Morioka, Obu, Aichi 474-8522, Japan; †Department of Demyelinating Disease and Aging, National Institute of Neuroscience, National Center of Neurology and Psychiatry, 4-1-1 Ogawa-higashi, Kodaira, Tokyo 187-8502, Japan; ‡Laboratory for Alzheimer's Disease, RIKEN Brain Science Institute, 2-1 Hirosawa, Wako-shi, Saitama 351-0198, Japan; §Department of Clinical Research, National Saigata Hospital, 468-1 Saigata, Ogata, Nakakubiki, Niigata 949-3193, Japan; and ¶Department of Neuropathology, Faculty of Medicine, University of Tokyo, 7-3-1 Hongo, Bunkyo-ku, Tokyo 113-0033, Japan

Corresponding author: Norifumi Watanabe, National Institute for Longevity Sciences, 36-3 Gengo, Morioka, Obu, Aichi 474-8522, Japan; E-mail: watanabn@nils.go.jp

ABSTRACT

Previous studies have suggested that heparan sulfate proteoglycans (HSPGs) play a role in deposition of β-amyloid protein (Aβ) in the Alzheimer's disease (AD) brain. In the present study, we demonstrated that glypican-1 can bind fibrillar Aβ, and the binding is mainly mediated by heparan sulfate (HS) chains. Further analysis revealed that glypican-1 is the major HSPG localized in detergent-insoluble glycosphingolipid-enriched (DIG) domains where all machineries for Aβ production exist and Aβ is accumulated as monomeric and oligomeric forms. Immunohistochemical studies demonstrated that glypican-1 is localized in primitive plaques as well as classic plaques. Moreover, overexpression of glypican-1 and amyloid precursor protein in SH-SY5Y cells resulted in reduced cell viability and made cells more susceptible to thapsigargin-induced stress and Aβ toxicity. The results raise the possibility that glypican-1 interacts with oligomerized or polymerized Aβ in such a specific compartment as DIG, resulting not only in amyloid deposition in senile plaques of AD brain, but also in accelerating neuronal cell death in response to stress and Aβ.

Key words: β-amyloid protein • SH-SY5Y cells • heparan sulfate proteoglycans

Alzheimer's disease (AD) is a neurodegenerative disorder characterized clinically by progressive dementia and memory loss and pathologically by neuronal and synaptic loss and extensive formation of neurofibrillary tangles (NFT), senile plaques, and vascular amyloid angiopathy (1, 2). The 39-43 amino acid peptide termed β-amyloid protein (Aβ) formed by proteolytic processing of the β-amyloid precursor protein (APP) is the major component of both senile plaques and cerebrovascular amyloid angiopathy (3, 4). The initial phase of amyloid

deposition is considered to be of importance in AD pathology, but the precise mechanism of Aβ accumulation in AD remains unclear.

Heparan sulfate proteoglycans (HSPGs) are ubiquitously present on the cell surface and in extracellular matrix, including the basement membrane (5, 6). HSPGs are subdivided into three categories: transmembrane type (syndecan), glycosylphosphatidylinositol (GPI)-anchored type (glypican), and matrix-associated type (perlecan, agrin, collagen type XVIII). HSPGs are known to interact with a variety of proteins such as antithrombin, growth factors, extracellular matrix components, selectins, and chemokines, through their heparan sulfate (HS) chains, thus contributing to the diverse biological activities (6). The structure of the sugar chains, especially sulfated ones within given sequences of the sugar residues, is important for such interactions (7–10).

The HSPG localized in senile plaques was first shown to be perlecan (11). Several in vitro and in vivo studies using mouse Engelbreth-Holm-Swarm (EHS) perlecan or HS chains have suggested that HSPGs may play a significant role in amyloid formation, for example, by promoting Aβ fibril formation or by protecting Aβ from protease degradation (12–19). It was reported that other HSPGs such as syndecan, glypican, and agrin are also present in senile plaques (20–23).

Although there have been a number of studies concerning the association between Aβ and HSPGs, they only demonstrated co-localization in plaques or binding ability of HSPGs derived from tissues other than the human brain. In the present study, we investigated the binding between HSPGs from the human brain and Aβ in vitro. We report here that 1) glypican-1 binds to Aβ and accumulates in detergent-insoluble glycosphingolipid-enriched (DIG) domains where Aβ is also concentrated, 2) overexpression of glypican-1 results in enhanced susceptibility of cells to a specific stress in the presence of Aβ, suggesting a possibility that glypican-1 plays a specific role in AD pathogenesis.

MATERIALS AND METHODS

Tissue samples

Brain tissues from patients with clinically diagnosed and neuropathologically confirmed AD (n=4, 4 females; age 77±8.6) and nondemented controls (n=4, 1 females and 3 males, age 70±2.9) were obtained at autopsy. Diagnosis of AD was based on a combination of neuropathological and clinical criteria. Tissue samples were snap-frozen in liquid nitrogen immediately after removal.

Antibodies and reagents

Mouse monoclonal antibody specific for synthetic Aβ1-16 (BAN50) was obtained from Takeda Chemical Industries, LTD (Osaka, Japan). Rabbit polyclonal antibodies specific for Aβ40 (FCA3340) and Aβ42 (FCA3542) were obtained from Dr. F. Checler (Institut de Pharmacologie Moleculaire et Cellulaire, CNRS, Valbonne, France). Rabbit polyclonal antibody Affi 28 was raised against the synthetic peptide corresponding to residues 1-28 of Aβ (24). Rabbit polyclonal antibody anti-C_{24} was raised against the synthetic peptide corresponding to residues 672-695 of APP (25). Mouse monoclonal antibodies against human glypican-1 (S1) or human syndecan-2

(10H4) were obtained from Dr. G. David (Center for Human Genetics, University of Leuven, Belgium). Mouse monoclonal antibody against human perlecan was purchased from ZYMED Laboratories, Inc. (South San Francisco, CA, USA). Mouse monoclonal antibody 3G10 and heparitinase (*Flavobacterium heparinum*) were purchased from Seikagaku Kogyo (Tokyo, Japan). Mouse monoclonal antibody specific for flotillin was purchased from BD Transduction Industries (Lexington, KY, USA). DEAE-Sepharose FF was purchased from Amersham Pharmacia Biotech (Uppsala, Sweden). Aβ (1-40) was purchased from Bachem Inc. (Torrance, CA, USA) and AnaSpec Inc. (San Jose, CA, USA). Fibrillar Aβ40 was prepared by incubating Aβ40 (in H_2O, 6 mg/ml) at 37°C for 5 days. Aβ (1-42) and Aβ (40-1) were purchased from AnaSpec Inc. All other reagents were of analytical grade.

Fractionation of human brain lysates

The brain tissues from control or AD subjects were homogenized in a solubilizing buffer comprising 4 M guanidine-HCl, 50 mM Tris-HCl (pH 8.0), 1% NP-40, 10 mM EDTA, 10 mM N-ethylmaleimide, and 1 mM PMSF at 4°C overnight. After centrifugation at 21,000 × g for 40 min, supernatants were dialyzed against a urea buffer comprising 7 M urea, 50 mM Tris-HCl (pH 7.4), 1% NP-40, 10 mM EDTA, 10 mM N-ethylmaleimide, and 1 mM PMSF. The lysates were subjected to a DEAE-Sepharose anion-exchange column (1.5×7.5 cm) and washed with the urea buffer. The bound materials were eluted with a linear NaCl gradient (0–2.25 M), and 150 fractions, 1 ml each, were collected.

Dot blotting assay

Samples were spotted onto nitrocellulose membranes directly or by using a Bio-Rad dot-blot apparatus according to the manufacturer's instructions. Blots were blocked with 5% nonfat milk in TBS (20 mM Tris-HCl, pH 7.4, 150 mM NaCl) and incubated with the primary antibody in TBS containing 0.05% Tween 20, 1% BSA, followed by incubation with appropriate horseradish peroxidase (HRP)-conjugated second antibodies. After washing, the blots were developed by the ECL detection system (NEN Life Science Products, MA, USA). The spots were quantitated using an image analyzer (LAS-1000plus, Fujifilm, Japan). For detection of HSPG with 3G10 mAb, blots were treated with 5 mU heparitinase at 37°C for 3 h before blocking. Aβ binding assay was carried out as follows: DEAE fractions were spotted onto nitrocellulose membranes as above. The membranes were treated or untreated with 5 mU heparitinase and incubated with fibrillar Aβ40 (1 μg/ml) at 4°C overnight. After washing, bound Aβ40 was detected with BAN50 or Affi 28 as above.

In vitro analysis of Aβ binding to HSPG

The fractions of DEAE-Sepharose chromatography or control brain lysates were incubated with 1 μg of fibrillar Aβ40 at 4°C overnight. After treatment with 2.5 mU heparitinase at 37°C for 3 h, samples were subjected to Western blotting with 3G10 mAb or anti-glypican-1 mAb.

Preparation of detergent-insoluble glycosphingolipid-enriched (DIG) fractions from human brains

DIG fractions were obtained according to an established protocol (26). The brain tissues from control or AD patients were homogenized in MES-buffered saline (MBS) (25 mM MES, pH 6.5, 0.15 M NaCl) containing 1% Triton X-100, 1 mM PMSF, 5 μg/ml pepstatin, and 5 μg/ml leupeptin. The sucrose concentration of the extract was adjusted to 40% by the addition of 80% sucrose in MBS; the extract was then placed at the bottom of an ultracentrifuge tube and overlaid with a 5%/35% discontinuous sucrose gradient in MBS without Triton X-100 (4 ml of 5% sucrose/4 ml of 35% sucrose). The gradients were centrifuged at 190,000 × g for 20 h in a SW41 rotor (Beckman, Palo Alto, CA). Twelve 1-ml fractions were collected from the top of the gradients.

Western blot

Western blot analysis of Aβ in each fraction was performed as follows. The fractions were subjected to TCA precipitation, and the resultant pellet was treated with chloroform/methanol (2:1), and then extracted with formic acid. Extracts were dried on Speed Vac and solubilized with the Laemmli sample buffer containing 7.5 M urea. The samples were separated on a 12% Tris-Tricine gel and then transferred to a nitrocellulose membrane (pore size 0.22 μm, Schleicher and Schuell, Dassel, Germany). The membrane was immersed in a boiling phosphate-buffered saline solution to enhance the detection sensitivity, and reacted with Aβ-specific antibodies. For Western blot analysis of other proteins, including glypican-1, proteins were separated on Tris-glycine SDS-PAGE and then transferred to a polyvinylidene difluoride membrane (Immobilon, Nihon Millipore Ltd., Yonezawa, Japan), and incubated with appropriate primary antibodies. Bound antibodies were detected using the ECL detection system.

Analysis of Aβ binding to HSPG in DIG fractions

The DIG fraction from control brains that did not contain detectable levels of Aβ was centrifuged at 98,000 × g for 40 min. The pellet was treated with chloroform/methanol (2:1), and then solubilized with 6 M guanidine-HCl, and the guanidine-soluble materials were spotted onto a nitrocellulose membrane. Aβ binding assay was carried out as described above.

Immunohistochemistry

Tissue preparation and immunohistochemical staining were performed as described previously (27–29). Briefly, the double immunohistochemical staining procedures were as follows. Thirty-μm-thick frozen sections were cut on a cryostat at −20°C, washed with 0.3% Triton X-100, and immersed in 15% sucrose in 0.01 M PBS at 4°C until staining. The sections were pretreated with 50 mU heparitinase diluted in 10 mM HEPES and 2 mM $CaCl_2$ (pH 7.0) at 37°C for 10 min, and then blocked with 5% goat serum in PBS. The sections were incubated with mouse monoclonal antibodies against perlecan (diluted 1:500), glypican-1(diluted 1:1000) or syndecan-2 (diluted 1:500) at 4°C for 24 h, then washed with 0.03% Tween 20 5 times for a total of 25 min, followed by incubation with a Texas red-conjugated anti-mouse IgG (Cappel, Boxtel, The Netherlands). The sections were blocked with 5% rabbit serum in PBS, and incubated with rabbit polyclonal antibodies specific for Aβ40 (FCA3340) or Aβ42 (FCA3542) at 4°C for 48 h,

followed by incubation with FITC-conjugated goat anti-rabbit IgG (Cappel) at 4°C for 12 h. To distinguish between primitive plaques and classical plaques, the sections were stained with 0.5% Congo red.

Construction of plasmids

To construct pTO-GPC1, pRS-GPC1 (kind gift from Dr. G. David) was digested with Hind III and Xba I. The 2 kb fragment was inserted into pcDNA4/TO (Invitrogen), which was digested with Hind III and Xba I.

Generation of tetracycline-responsive gene-inducible cell lines

Cells were cultured in D-MEM/F-12 (Gibco-BRL, Grand Island, NY) containing 10% fetal bovine serum (Equitech-BIO, Inc., Kerrville, TX) unless otherwise indicated. SH-SY5Y cells or SH-SY5Y cells, which were stably transfected with Swedish mutant APP (sweAPP-SH cells), were cotransfected with pcDNA6/TR (Invitrogen) and pcDNA4/TO or pTO-GPC1 using CellPhect Transfectant kit (Amersham Pharmacia Biotech, Piscataway, NJ) according to the manufacturer's protocol. Two days after transfection, transfectants were subcultured and selected in culture media supplemented with 4 μg/ml blasticidin and 300 μg/ml Zeocin. Induction of glypican-1 expression in the presence of 1 μg/ml tetracycline in each selected clone was confirmed by Western blotting.

Cell viability analysis by WST assay

Cells were plated at 1×10^4 cells/well in 96-well plates and incubated with or without 1 μg/ml tetracycline for various periods of time (for 0–4 days). After removal of medium, 100 μl of WST-1 solution (Chemicon International Inc., Temecula, CA) was added to each well. The plates were incubated further for 4 h at 37°C, and the optical density at 450 nm was measured with a microplate reader (Model 550, Bio-Rad Laboratories, Hercules, CA).

Treatment of cells with stress-inducing reagents or Aβ

Cells were plated at 1×10^4 cells/well in 96-well plates, and the next day cultured in medium supplemented with 1% FBS (±tetracycline) for stress inducing experiments or medium supplemented with 10% FBS (±tetracycline) for Aβ treatment. After overnight incubation, medium was replaced with 1% FBS medium (±tetracycline) containing various concentrations of stress-inducing reagents or 10% FBS medium (±tetracycline) containing various concentrations of Aβ. After overnight incubation in the case of stress response or 4 days incubation in that of Aβ treatment, cell viability was analyzed as described above.

ELISA

Equal protein amounts of DIG fractions from each human brain were subjected to TCA precipitation. The pellets were then lysed in 15 μl of 70% formic acid at 4°C overnight. The samples were neutralized by adding 285 μl 2 M Tris-HCl. Insoluble material was pelleted by centrifugation, and the supernatant was diluted 1:2 in H_2O. Quantification of Aβ in 100 μl aliquot was performed by using Human β Amyloid ELISA Kit (Biosource International,

Camarillo, CA) according to the manufacturer's protocol. Quantification of glypican-1 and flotillin was performed as follows. Proteins were immobilized in 96-well microtiter plates by adding 50-μl aliquots to wells at 4°C overnight. After washing and blocking, wells were incubated with 3 μg/ml anti-human glypican-1 mAb (S1) or anti-flotillin antibody at 4°C overnight, followed by incubation with HRP-labeled secondary antibody at room temperature for 2 h. After washing, wells were incubated with tetramethylbenzidine (TMB) solution at room temperature for 30 min. The reaction was terminated by addition of 1.8 N H_2SO_4, and the plate was read at 450 nm in a microplate reader.

RESULTS

Binding of Aβ to HSPG(s) derived from human brains

To identify HSPGs derived from the human brain with the capacity to bind Aβ, control human brain lysates were separated using anion exchange DEAE-Sepharose chromatography. The dot blotting assay using 3G10 mAb, which is specific to neoepitope on HSPGs generated by heparitinase treatment, revealed that fractions 55–61 contained HSPGs (Fig. 1*A*). Endogenous Aβ could not be detected with anti-Aβ antibody (BAN50) in any fraction (data not shown). Fractions containing possible Aβ binding protein(s) were subsequently determined by the Aβ binding assay. In this assay, DEAE fractions were spotted onto nitrocellulose membranes, and after incubation with fibrillar Aβ, the bound Aβ was detected with anti-Aβ antibody. As shown in Fig. 1*B* and *C*, the fractions containing HSPGs exclusively showed the binding activity to fibrillar Aβ. Pretreatment of the blot with heparitinase resulted in a marked decrease in Aβ binding, indicating that this binding was mainly dependent on HS chains.

Identification of glypican-1 as an Aβ binding HSPG from human brain

Previous studies reported that Aβ binding to HS chains prevents heparanase-catalyzed degradation of HS chains (18). Thus, we examined whether preincubation of the DEAE fractions having the Aβ binding activity with Aβ alters the sensitivity of HSPGs in these fractions to heparitinase treatment. In the absence of preincubation with Aβ, several bands (~200 kDa, ~100 kDa, ~60 kDa, ~40 kDa) were detected with 3G10 mAb in the DEAE fractions, indicating that they contained plural HSPGs (Fig. 2*A*, lane 1). Preincubation with Aβ resulted in the obvious disappearance of the ~60 kDa band, while the intensity of the other bands was relatively unchanged (Fig. 2*A*, lane 2). This result suggested that an HSPG with the ~60 kDa core protein bound to Aβ preferentially and this binding prevented heparitinase-catalyzed degradation of HS chains. Glypicans are presently known as HSPGs with a ~60 kDa core protein and 6 glypicans (glypican-1 to -6) have been cloned (30). Among them, glypican-1 is the major HSPG expressed in the adult brain (31, 32). Therefore, we examined whether the Aβ binding DEAE fractions contain glypican-1 using dot blotting assay (Fig. 1*C*) and obtained a result indicating that they contained glypican-1. In addition, the reactivity profile of this mAb was in good accordance with that of 3G10 mAb, suggesting that glypican-1 was a major Aβ binding HSPG in these fractions. We next performed the same incubation experiments to clarify the identity of the ~60 kDa band using anti-glypican-1 mAb. A 60-kDa band of glypican-1 core protein was detected in the lysates (Fig. 2*B*, lane 1), and preincubation of the lysates with Aβ resulted in a marked decrease of this 60 kDa band and the appearance of a smear band (>100 kDa) probably representing intact

glypican-1 (Fig. 2*B*, lane 2). Pretreatment of lysates with heparitinase before incubation with Aβ recovered the 60 kDa band, suggesting that Aβ was unable to bind to heparitinase treated glypican-1 (Fig. 2*B*, lane 4). These results suggest that glypican-1 derived from the human brain can bind to Aβ in an HS chain dependent manner.

Aβ binding to glypican-1 depends on its aggregation state

It was reported that heparin or mouse EHS HSPG binds fibrillar Aβ (fAβ) but not non-fibrillar Aβ (non-fAβ) with high affinity (17, 33). In the present in vitro analysis of Aβ binding to glypican-1, the core protein of glypican-1 could be detected after incubation with non-fibrillar Aβ but not after with fibrillar Aβ at similar levels to those observed in the non-treated sample, suggesting that non-fibrillar Aβ had no or little binding ability to glypican-1 (Fig. 2*C*). In support of this, binding of non-fibrillar Aβ to HSPGs was not observed on dot blot membranes (data not shown).

Glypican-1 is a major HSPG in DIG domains from human brains

Glypican-1 is a GPI-anchored HSPG, and most, if not all, GPI-anchored proteins are localized in special membrane domains called detergent-insoluble glycosphingolipid-enriched (DIG) domains (34–36). Therefore, we next examined whether glypican-1 is present in the DIG fraction from brain tissues. The DIG was recovered in fractions 4–6, into which flotillin, a marker protein of DIG, was exclusively fractionated. Western blotting with anti-glypican-1 showed that glypican-1 was mainly present in fraction 5, indicating the localization of glypican-1 to the DIG domains (Fig. 2*D*). Moreover, Western blotting with 3G10 mAb indicated that HSPGs other than glypican-1 were almost undetectable in the DIG fraction (Fig. 2*E*). In addition, glypican-1 was almost completely recovered in the pellet after centrifugation of the DIG fraction (data not shown). In the present analysis, we found that DIG fractions from certain control brain tissues did not contain detectable amounts of Aβ. Such DIG fractions can be used to examine direct binding between Aβ and glypican-1 by dot blotting assay. An insoluble pellet from the DIG fraction was solubilized with 6 M guanidine-HCl, and the solubilized sample was used for dot blot Aβ binding assay. As shown in Fig. 2*F*, Aβ bound to guanidine soluble samples from the DIG fraction, and this binding was significantly inhibited by heparitinase pretreatment, indicating that Aβ could bind to DIG-resided glypican-1 in an HS chain dependent manner.

Co-localization of glypican-1 and Aβ in DIG fractions from AD brain

Recently, DIG domains or "rafts" have received attention with regard to the pathogenesis of AD, because accumulation of Aβ in these domains was demonstrated and appeared to correlate with the extent of Aβ deposition in the brain (37–39). Thus, it is possible that glypican-1 also participates in the process of Aβ accumulation by interaction with Aβ in such specific microdomains. To clarify this possibility, we examined whether glypican-1 and Aβ are co-fractionated in DIG fractions from AD brains. The fractions were analyzed by Western blots with antibodies to human glypican-1, Aβ, Aβ40, Aβ42, or APP. Glypican-1 was recovered mainly in DIG fractions (Fig. 2*G*), confirming our earlier result (Fig. 2*D*). Full length APP was fractionated predominantly in the high-density fractions, and to a smaller extent in DIG fractions. Importantly, we observed that significant amounts of Aβ40 and Aβ42 were present in the DIG

fractions as monomers and SDS-stable dimers (Fig. 2G). Interestingly, BAN50, of which epitope is located in Aβ1-10, labeled Aβ monomers much stronger than Aβ dimers, suggesting that these SDS-stable dimers were formed in a way that the N-terminal portion of Aβ was masked, modified, or deleted.

Preferential role of glypican-1 in Aβ42 accumulation in DIG domains

Given that Aβ binds to glypican-1 and these two proteins were accumulated in DIG domains, it is possible that there is a correlation between them. To examine this possibility, we quantified the levels of Aβ and glypican-1 in the DIG fraction using ELISA, and the results were plotted. Interestingly, there was a strong correlation between Aβ42 and glypican-1 (ctrl; r=0.9517, AD; r=0.8756), while no correlation between Aβ40 and glypican-1 (ctrl; r=0.3559, AD; r=0.0854) was observed (Fig. 2H). These results suggest that glypican-1 plays a preferential role in an accumulation of Aβ42 in DIG domains.

Co-localization of glypican-1 in primitive-type plaques

To clarify whether glypican-1 and other HSPGs contribute to AD pathology in more detail, we performed double immunohistochemical staining of plaques at different stages. To distinguish primitive plaques from classic plaques, Congo red staining was performed (data not shown). Both primitive (indicated by arrows) and classic plaques (indicated by arrowheads) in AD brains were stained with either anti-Aβ40 or anti-Aβ42 antibody (Fig. 3A, D, G, and J). Co-localization of glypican-1 staining was observed in classic senile plaques with an amyloid core (Fig. 3B, C, E, and F). In addition, primitive plaques, which were Congo red-negative and considered to be at an earlier phase in the plaque formation process, were also stained with anti-glypican-1 mAb (Fig. 3B and C, arrows), suggesting that glypican-1 is involved in the initial stage of plaque formation. We investigated 24 plaques and found that ~90% was positive for both Aβ and glypican-1. On the other hand, syndecan-2 staining was observed only in classic plaques but not in primitive plaques (Fig. 3H, I, K, and L). Consistent with previous findings (20–23), perlecan staining was not observed in senile plaques (data not shown). Altogether, these results raise the possibility that glypican-1 has a distinct role in the Aβ deposition from the early phase of plaque formation.

Effect of glypican-1 overexpression on cell viability

To explore the function of glypican-1 other than plaque formation, we generated transfectants which overexpressed glypican-1 in a tetracycline-inducible manner. Western blot analysis showed that the transfectants were induced to express a large amount of glypican-1 protein when cultured with tetracycline (Fig. 4A). Time course experiment demonstrated that induction of glypican-1 expression was begun 5 min after addition of tetracycline and reached maximal levels after 12 h. On the basis of scanning densitometry, addition of tetracycline resulted in a greater than 300-fold induction of glypican-1. Cell viability of these cells with or without the induction of glypican-1 was analyzed using WST assay. As shown in Fig. 4, overexpression of glypican-1 decreased viability of cells co-expressing APP carrying Swedish mutation of familial Alzheimer's disease (Fig. 4Bc). On the other hand, neither glypican-1 nor Swedish APP overexpression alone affected cell viability (Fig. 4Ba, b). Because the production of Aβ in

Swedish APP-expressing cells was largely increased, it is possible that the observed effect of glypican-1 on cell viability was due to enhanced Aβ toxicity by binding to glypican-1. To examine this, transfectants were cultured with exogenously added Aβ for 4 days, and then cell viability was measured. The viability of all cells examined was not affected by adding non-fAβ40, fAβ40, or Aβ40-1 even though glypican-1 expression was induced (Fig. 4*Ca–f, j–l*). In contrast, Aβ42 significantly reduced cell viability only when glypican-1 was overexpressed (Fig. 4*Cg, i*). These results indicate that cells that overexpress glypican-1 become more susceptible to Aβ42 toxicity, resulting in enhanced cell death.

Effect of glypican-1 overexpression on ER stress

It was reported that ER stress is an important factor in the neuropathology of a wide variety of neurological disorders, including AD (40, 41). Studies have shown that neurotoxicity elicited by Aβ is at least partially mediated by ER stress (42–44), raising a possibility that the ER stress response is influenced by overexpression of glypican-1, which may result in enhanced susceptibility of cells to Aβ42 toxicity. Therefore, we next examined the effect of glypican-1 expression on the stress response. As ER stress inducers, we used thapsigargin, a well-established proapoptotic agent, which increases the intracellular Ca^{2+} concentration through inhibition of the ER Ca^{2+}/Mg^{2+}-ATPase (45), tunicamycin, an inhibitor of core glycosylation, and brefeldin A, an agent that blocks vesicular trafficking from the ER to the Golgi apparatus. Cell death induced by thapsigargin was accelerated when glypican-1 was overexpressed in cells co-expressing Swedish APP (Fig. 4*Dc*). However, such an acceleration was not observed in cells which expressed glypican-1 or Swedish APP alone (Fig. 4*Da, b*). On the other hand, the stress response by tunicamycin and brefeldin A did not alter the cell survival even though cells were co-expressing Swedish APP and glypican-1 (Fig. 4D, *d–i*). These results suggest that glypican-1, together with Aβ, makes cells more vulnerable to certain, but not all stresses.

DISCUSSION

In this study, we performed biochemical analyses to identify human brain HSPG that can bind Aβ and demonstrated, for the first time, that glypican-1 possesses binding ability to Aβ. We also found that this binding was mainly dependent on HS chains and made HS chains resistant to heparitinase. Importantly, glypican-1 was localized predominantly in DIG domains where accumulation of Aβ was also observed, raising the possibility that glypican-1 interacts with Aβ in such specific microdomains. This is supported by the findings that Aβ42 levels were in good correlation with glypican-1 levels in DIG domains. Moreover, the present immunohistochemical analyses showed that glypican-1 was localized in primitive plaques as well as in classic plaques, while another HSPG (syndecan-2) was present only in plaques with an amyloid core, implying that glypican-1 plays a role in the initial phase of amyloid plaque formation. Although HSPGs are co-localized in senile plaques and may promote amyloid formation, deposition, and/or persistence by binding to Aβ (12–19), it remains uncertain how HSPGs are involved in AD pathogenesis and which HSPG has a pathogenic role in AD. The findings of the present study may suggest that glypican-1 plays a specific and distinct role. First, glypican-1 had higher affinity to Aβ than other HSPGs since HS chains on glypican-1 became preferentially resistant to heparitinase after incubation with Aβ. The present in vitro binding assay also showed the specific binding between glypican-1 and Aβ. The higher binding affinity of glypican-1 to Aβ